Pramana – J. Phys. (2020) 94:65
https://doi.org/10.1007/s12043-020-1932-y

Long-lived quantum coherence in a two-level semiconductor quantum dot

D A M ABO-KAHLA[1,2]

[1]Department of Mathematics, Faculty of Science, Taibah University, Medina, Kingdom of Saudi Arabia
[2]Department of Mathematics, Faculty of Education, Ain Shams University, Roxy, Cairo, Egypt
E-mail: doaa_abukahla@ymail.com

MS received 1 March 2019; revised 26 December 2019; accepted 16 January 2020;
published online 16 April 2020

Abstract. In this paper, we present an analytical solution for the system of two-level semiconductor quantum dot. In addition, we discuss the rates of the photon radiative and phonon radiationless transitions from the excited state (α_{12}, α_{21}), the rate of processes of pure dephasing (γ), the detuning parameter (Δ) and the Rabi frequency (Ω), on the atomic occupation probabilities ($\rho_{11}(t)$ and $\rho_{22}(t)$), the atomic population inversion ($\rho_z(t)$), the purity ($P_A(t)$), the von Neumann entropy ($S(t)$) and the information entropies ($H(\sigma_x)$, $H(\sigma_y)$ and $H(\sigma_z)$). We clearly observe the emergence of long-lived quantum coherence phenomenon in all the curves for some special cases of α_{12}, α_{21}, γ, Δ and Ω. Besides, the decay phenomenon is quite evident in the purity curves, which can be simply controlled by changing the values of α_{12}, α_{21} and γ.

Keywords. Semiconductor; quantum dot; long-lived quantum coherence.

PACS Nos 42.50.−p; 03.67.−a

1. Introduction

The materials, broadly speaking, were divided into three main categories: the conductors [1] that allow electrons to flow through them, the insulators [2] that do not allow the flow of electrons and semiconductors [3–7] that allow the flow of electrons only under certain conditions. Perhaps the best explanation for the difference between them is the difference in their band gaps [8–10]. Defined as a range of energy in matter, the band gap does not contain any electrons within. Conductors [1,11], such as metals including iron, copper, silver, gold and aluminum, have no band gaps. So, electrons can move freely through them, and thus the electric current can be easily connected. Insulators [2,12,13], such as oil, glass, rubber and ceramics, have large band gaps that restrain the flow of electrons. In contrast [3–7], semiconductors contain small band gaps, and so the flow of electrons and electronic holes can be controlled by adding impurities to the material. The properties of semiconductors [14–16] depend on their degree of purity. Semiconductors are divided into pure elements, such as silicon or germanium, and non-pure elements, such as gallium arsenide compounds or cadmium selenide [17–20]. Non-pure elements are generated by adding small amounts of impurities to pure semiconductors, through a process called doping, which leads to significant changes in the properties of the elements [14–16]. Some properties of the semiconductor materials were discovered during the mid-19th century and the early decades of the 20th century [21–23]. In 1874, the first practical application of semiconductors in electronics was discovered by Braun [24], when he created a diode, which is a semiconductor device with two terminals allowing the flow of current in one direction only. At the beginning of the 20th century, G W Pickard created the first commercially available semiconductor, branded as the 'cat's-whisker detector', a primitive semiconductor diode, used in early radio receivers [21–23]. Semiconductors were then used only as two-terminal devices, such as rectifiers and photodiodes [21–23]. In 1947, developments in quantum physics led to the development of the transistor [18,25,26]. In 1958, Sterling developed integrated circuits [27]. The main objective of this work was to condense more components in a much smaller space to achieve higher speed and lesser cost.

The development of this work subsequently allowed us to build calculators, flight control systems ipads and most of the modern technological devices.

Our study focusses on semiconductor quantum dots [28–33], which are very small semiconductor particles [3–7,14–18,25,26,34–36]. Their size is measured by nanometre, and so their optical and electronic properties [37–40] are different from those of the larger LED molecules. In 1981, Russian physicist Alexey I Ekimov discovered quantum dots. He discovered that they are small nanoparticles whose diameter ranged from 2 nm (nanometers) to 10 nm, and that the colour of these particles varies by their size [28–33]. Quantum dots are sometimes referred to as artificial atoms. This expression confirms that a quantum dot is a single object with bound, discrete electronic states, that is, very similar to atoms or molecules that occur naturally [41–43]. Quantum dots can also be classified into different types based on their composition and structure. Many types of quantum dots emit light for specific frequencies, if light or electricity is directed to them. These frequencies can be precisely tuned, by changing the size of the dots, which has led to the emergence of many applications [28,44–58], including quantum computing, medical imaging, solar cells, LED lamps, diode lasers and transistors [18,25,26]. Besides, the highly tunable properties of quantum dots make them crucially vital in a wide variety of research and commercial applications in biochemistry, biometric sensing [36], Langmuir–Blodgett thin films [59–61] and spin-coating [62].

Because of the above-mentioned importance of this field, our study is solving the master equation for the density matrix $\rho(t)$ of the two-level semiconductor quantum dot, as an example of an artificial atom. Although this problem has been almost covered in physics from the theoretical and experimental perspectives [63–66], the research in this vital area still lacks the mathematical treatment. Hence, after reviewing the previous studies, we think that our mathematical solution in this paper would represent a whole new endeavor that may provide different explanatory points of view to the equations of semiconductors systems. The importance of this mathematical study is also emphasised by several phenomena which have been revealed through the processing of the system, including the phenomenon of long-lived quantum coherence and the decay phenomenon. These phenomena, as we shall see later, make us control the behaviour of the system by changing the parameters over time. This can help greatly in the laboratory experiments and in many applications of this field.

Accordingly, as an application to solve this system, we calculate the atomic inversion, the purity and the entropies. The atomic inversion is one of the most important quantities, and is defined as 'the difference between the probabilities of finding the atoms in their excited states and in their ground states' [67,68]. While the purity is an indicator of the degree of influence of the field on the atom, and the range of its value is between 0 and $(1 - 1/d)$, 0 refers to a completely pure state, and $(1 - 1/d)$ refers to a completely mixed state (here, d is the dimension of the density matrix) [67]. On the other hand, the entropy is a measure that determines the amount of information missing from the system. It is also a measure of the degree of chaos in the system, as a result of the effect of the field or the surrounding environment on this system [69–72].

This paper is organised as follows: in §2 we describe the Hamiltonian of the system in question, two-level semiconductor quantum dot, and we obtain the explicit analytical solution of this model. In §3, we discuss the atomic occupation probabilities ($\rho_{11}(t)$ and $\rho_{22}(t)$), the atomic population inversion ($\rho_z(t)$) and the time evolution of the purity ($P_A(t)$), by changing the rates of the photon radiative and phonon radiationless transitions from the excited state (α_{12}, α_{21}), the rate of the processes of pure dephasing (γ), the detuning parameter (Δ) and the Rabi frequency (Ω). In §4, we discuss the time evolution of the von Neumann entropy ($S(t)$) and the information entropies ($H(\sigma_z)$, $H(\sigma_y)$ and $H(\sigma_x)$). Finally, conclusions are given at the end of the paper.

2. The model

We discuss a two-level semiconductor quantum dot as an example of an artificial atom with the energy splitting ω_0 between the ground ($|-\rangle$) and the excited ($|+\rangle$), states. The semiconductor quantum dot is affected by a coherent laser field with frequency (ω_L). The master equation for the density matrix ($\rho(t)$) of the system under study is as follows [73–75]:

$$i\frac{\partial\rho(t)}{\partial t} = [H, \rho(t)] + i\Gamma\rho(t), \tag{1}$$

where

$$H = \Delta\sigma_z + \frac{\Omega}{2}(\sigma_+ + \sigma_-), \tag{2}$$

Planck's constant $\hbar = 1$ is the Hamiltonian of the system in the rotating wave approximation [76–79] and

$$\Gamma\rho(t) = \frac{\alpha_{21}}{2}F[\sigma_-]\rho(t) + \frac{\alpha_{12}}{2}F[\sigma_+]\rho(t) + \frac{\gamma}{2}F[\sigma_z]\rho(t), \tag{3}$$

is the relaxation superoperator. σ_+, σ_- and σ_z are the Pauli spin operators which describe the states of the

two-level semiconductor quantum dot. These satisfy the following commutation relationships:

$$[\sigma_+, \sigma_-] = 2\sigma_z, \quad [\sigma_z, \sigma_\pm] = \pm\sigma_\pm. \tag{4}$$

Here Ω, the Rabi frequency, is an indicator of the strength of the interaction of our system with the laser field, $\Delta = \omega_0 - \omega_L$ is the detuning parameter, α_{12} and α_{21} are the rates of the photon radiative and phonon radiationless transitions FROM the excited state, $|+\rangle$, to the ground state, $|-\rangle$ and vice versa and γ is the rate of the processes of pure dephasing.

As for $F[\sigma_{\pm,z}]$, we can define the function F of any operator U as follows:

$$F[U]\rho(t) = 2U\rho(t)U^\dagger - U^\dagger U\rho(t) - \rho(t)U^\dagger U. \tag{5}$$

After long calculations, we can write the master equation (1) as follows:

$$\begin{aligned}
\frac{\partial\rho_{11}}{\partial t} &= i\frac{\Omega}{2}(\rho_{12} - \rho_{21}) - \alpha_{21}\rho_{11} + \alpha_{12}\rho_{22},\\
\frac{\partial\rho_{22}}{\partial t} &= -i\frac{\Omega}{2}(\rho_{12} - \rho_{21}) + \alpha_{21}\rho_{11} - \alpha_{12}\rho_{22},\\
\frac{\partial\rho_{12}}{\partial t} &= -\left(i\Delta + \frac{\alpha_{21}}{2} + \frac{\alpha_{12}}{2} + \frac{\gamma}{4}\right)\rho_{12}\\
&\quad + i\frac{\Omega}{2}(\rho_{11} - \rho_{22}),\\
\frac{\partial\rho_{21}}{\partial t} &= \left(i\Delta - \frac{\alpha_{21}}{2} - \frac{\alpha_{12}}{2} - \frac{\gamma}{4}\right)\rho_{21}\\
&\quad - i\frac{\Omega}{2}(\rho_{11} - \rho_{22}),
\end{aligned} \tag{6}$$

where ρ_{11} and ρ_{22} are the diagonal elements (the atomic occupation probabilities), while ρ_{12} and ρ_{21} are the off-diagonal elements (coherences) of the two-level semiconductor quantum dot. We can rewrite the system of equations (6) by using the components of the density operator $\rho(t)$, $\rho_x(t)$, $\rho_y(t)$ and $\rho_z(t)$, as follows:

$$\begin{aligned}
\frac{\partial\rho_x(t)}{\partial t} &= -S\rho_x(t) - \Delta\rho_y(t),\\
\frac{\partial\rho_y(t)}{\partial t} &= \Delta\rho_x(t) - S\rho_y(t) + \Omega\rho_z(t),\\
\frac{\partial\rho_z(t)}{\partial t} &= -\Omega\rho_y(t) - Q\rho_z(t),
\end{aligned} \tag{7}$$

where

$$\begin{aligned}
\rho_x(t) &= \rho_{12}(t) + \rho_{21}(t),\\
\rho_y(t) &= -i(\rho_{21}(t) - \rho_{12}(t)),\\
\rho_z(t) &= \rho_{22}(t) - \rho_{11}(t)
\end{aligned} \tag{8}$$

and

$$\begin{aligned}
S &= \alpha_{12} + \frac{\gamma}{4},\\
Q &= 2\alpha_{12}, \quad \alpha_{12} = \alpha_{21}.
\end{aligned} \tag{9}$$

We initially take the atom in the following superposition state:

$$|\Psi(0)\rangle = \sin\left(\frac{\theta}{2}\right)\exp(-i\varphi)\,|1\rangle + \cos\left(\frac{\theta}{2}\right)|2\rangle\,, \tag{10}$$

where $|1\rangle$ ($|2\rangle$) is the ground (excited) state of the atom. Here $\varphi \in [0, 2\pi]$ is the relative phase between the ground and the excited states and $\theta \in [0, \pi]$ denotes the initial coherence of the two levels.

However, the system initially is defined as follows [80]:

$$\rho(0) = |\Psi(0)\rangle\langle\Psi(0)|\,, \tag{11}$$

where

$$\begin{aligned}
\langle\Psi(0)| &= \text{the complex conjugate of } |\Psi(0)\rangle\\
&= (|\Psi(0)\rangle)^\dagger.
\end{aligned} \tag{12}$$

Hence, we get the following equations:

$$\begin{aligned}
\rho_{11}(0) &= \langle 1|\,\rho(0)\,|1\rangle = \sin^2\left(\frac{\theta}{2}\right),\\
\rho_{22}(0) &= \langle 2|\,\rho(0)\,|2\rangle = \cos^2\left(\frac{\theta}{2}\right),\\
\rho_{12}(0) &= \langle 1|\,\rho(0)\,|2\rangle = \frac{1}{2}\sin(\theta)\exp(-i\varphi),\\
\rho_{21}(0) &= \langle 2|\,\rho(0)\,|1\rangle = \frac{1}{2}\sin(\theta)\exp(i\varphi).
\end{aligned} \tag{13}$$

But

$$\begin{aligned}
\rho_x(0) &= \rho_{12}(0) + \rho_{21}(0),\\
\rho_y(0) &= -i(\rho_{21}(0) - \rho_{12}(0)),\\
\rho_z(0) &= \rho_{22}(0) - \rho_{11}(0).
\end{aligned} \tag{14}$$

This means that the initial conditions of this system are

$$\begin{pmatrix}\rho_x(0)\\ \rho_y(0)\\ \rho_z(0)\end{pmatrix} = \begin{pmatrix}\sin\theta\cos\varphi\\ \sin\theta\sin\varphi\\ \cos\theta\end{pmatrix}. \tag{15}$$

We can solve the system of equations (7) by Laplace transformation and obtain the following solutions:

$$\begin{aligned}
\rho_x(t) &= \sum_{i=1}^{3}\frac{X\exp(t\lambda_i)}{(\lambda_i - \lambda_j)(\lambda_i - \lambda_k)}, \quad i \neq j \neq k,\\
&\quad j, k = 1, 2, 3,\\
\rho_y(t) &= \sum_{i=1}^{3}\frac{Y\exp(t\lambda_i)}{(\lambda_i - \lambda_j)(\lambda_i - \lambda_k)}, \quad i \neq j \neq k,\\
&\quad j, k = 1, 2, 3,\\
\rho_z(t) &= \sum_{i=1}^{3}\frac{Z\exp(t\lambda_i)}{(\lambda_i - \lambda_j)(\lambda_i - \lambda_k)},
\end{aligned}$$

$$i \neq j \neq k, \quad j,k = 1,2,3, \tag{16}$$

where

$$\begin{aligned} X &= \rho_x(0)\{\lambda_i^2 + (S+Q)\lambda_i + SQ + \Omega^2\} \\ &\quad +\rho_y(0)\Delta(\lambda_i + Q) + \rho_z(0)\Delta\Omega, \\ Y &= -\rho_x(0)\Delta(\lambda_i + Q) + \rho_y(0) \\ &\quad \times\{\lambda_i^2 + (S+Q)\lambda_i + SQ\} + \rho_z(0)\Omega(S+\lambda_i), \\ Z &= \rho_x(0)\Delta\Omega + \rho_y(0)\Omega(S+\lambda_i) \\ &\quad +\rho_z(0)\{\lambda_i^2 + 2S\lambda_i + (S^2+\Delta^2)\} \end{aligned} \tag{17}$$

and

$$\begin{aligned} \lambda_1 &= \frac{1}{6}\Bigg\{ -2(2S+Q) - \frac{2^{4/3}A}{(\sqrt{C}+B)^{1/3}} \\ &\quad +2^{2/3}(\sqrt{C}+B)^{1/3}\Bigg\}, \\ \lambda_2 &= \frac{1}{6}\Bigg\{ -2(2S+Q) + \frac{2^{4/3}A(i\sqrt{3}+1)}{(\sqrt{C}+B)^{1/3}} \\ &\quad +2^{2/3}(i\sqrt{3}-1)(\sqrt{C}+B)^{1/3}\Bigg\}, \\ \lambda_3 &= \tilde{\lambda}_2 \text{ (the complex conjugate of } \lambda_2), \end{aligned} \tag{18}$$

where

$$\begin{aligned} A &= 3(\Delta^2+\Omega^2) - (S-Q)^2, \\ B &= (S-Q)(2S^2 - 4SQ + 2Q^2 + 18\Delta^2 - 9\Omega^2), \\ C &= (S-Q)^2\{2[(S-Q)^2 + 9\Delta^2] - 9\Omega^2\}^2 \\ &\quad -4\{(S-Q)^2 - 3(\Delta^2+\Omega^2)\}^3. \end{aligned} \tag{19}$$

As applications to the solution of our system, we discuss the atomic occupation probabilities ($\rho_{11}(t)$ and $\rho_{22}(t)$), the atomic inversion ($\rho_z(t)$), the purity ($P_A(t)$), the von Neumann entropy ($S(t)$) and the information entropies ($H(\sigma_x)$, $H(\sigma_y)$ and $H(\sigma_z)$), of the semiconductor quantum dot. In addition, we study the dephasing rate in the zeroth approximation [81] in $\max\{\alpha_{12}, \alpha_{21}, \gamma\}/\Omega$, at the end of the discussion.

3. Results and discussion

3.1 *The atomic population inversion and the purity*

Based on the analytical solution of a two-level semiconductor system in the previous section, we investigate the evolution in time of $\rho_{11}(t)$, $\rho_{22}(t)$ and $\rho_z(t)$, which is given by [67,68]

$$P_A(t) = \mathrm{Tr}_A(\rho_A^2(t)) \tag{20}$$

$$= \rho_{11}^2 + 2\,|\rho_{12}|^2 + \rho_{22}^2, \tag{21}$$

where ρ_A, the density matrix of the atom and ρ_{ij}, $i, j = 1, 2$, the solution obtained from eqs (6), are the elements of the matrix ρ_A, because of the afore-solved system of eqs (6) were actually handling the system of the semiconductor quantum dot only that has already been affected by a coherent laser field with the frequency ω_L.

In the numerical results, we consider the initial coherence of the two levels $\theta = 0$ and the relative phase between the excited and ground states $\varphi = 0$ (this means that initially the semiconductor system will be in the excited state, $\rho_{22}(0) = 1$, $\rho_{11}(0) = \rho_{12}(0) = \rho_{21}(0) = 0$). In figures 1–6, we can observe clearly the emergence of the phenomenon of long-lived quantum coherence [82–85]. This phenomenon means that the curve after a certain period of time and at a certain value becomes fixed, wherein the influence of the parameters fades away. In other words, the curve after some fluctuation becomes fixed, without any influence of time. In figure 1, we investigate the effects of α_{12}, α_{21} and γ on $\rho_{11}(t)$, $\rho_{22}(t)$, $\rho_z(t)$ and $P_A(t)$, when $\Omega = 10$ and $\Delta = 10$. At $\alpha_{12} = \alpha_{21} = \gamma = 0.1$, $\alpha_{12} = \alpha_{21} = \gamma = 0.5$ and $\alpha_{12} = \alpha_{21} = \gamma = 0.9$, both the curves of $\rho_{11}(t)$ and $\rho_z(t)$ start from their minimum values at $\rho_{11}(t) = 0$, $\rho_z(t) = -1$, while the curves of $\rho_{22}(t)$ start with their maximum value at $\rho_{22}(t) = 1$. In the beginning, we note that the three curves of $\rho_{11}(t)$, $\rho_{22}(t)$ and $\rho_z(t)$ have many oscillations of great intensity and amplitude. However, after a certain period of time, we find that the intensity, the amplitude and the number of oscillations become significantly less. So the curves take the shape of a fixed straight line, and we find that the increase in α_{12}, α_{21} and γ causes a faster decrease in the number of oscillations and their intensity and amplitude, thereby, turning the curves quickly to straight lines after a short period of time. As for the purity curves, $P_A(t)$, they start from their maximum value at $P_A(t) = 1$, then suddenly decrease clearly to show an evident decay. By increasing α_{12}, α_{21} and γ, this decay is greater and faster, until the curves become fixed at $P_A(t) = 0.5$, where the curve is in completely mixed state. We also notice an apparent phenomenon of long-lived quantum coherence. In figure 3, we investigate the effects of Δ on $\rho_{11}(t)$, $\rho_{22}(t)$, $\rho_z(t)$, $P_A(t)$, when $\Omega = 10$ and $\alpha_{12} = \alpha_{21} = \gamma = 0.3$. At $\Delta = 5$, 15 and 25, the curves of $\rho_{11}(t)$ and $\rho_z(t)$ start from their minimum values, then increase significantly until they reach their maximum values, while the curves of $\rho_{22}(t)$ start from their maximum value, then, after a certain period of time, decrease significantly until they reach their minimum values. By increasing Δ, all the curves, $\rho_{11}(t)$, $\rho_{22}(t)$ and $\rho_z(t)$, are in the fixed states, where the amplitudes of the curves are gradually reduced significantly, and this transforms the curves to fixed straight

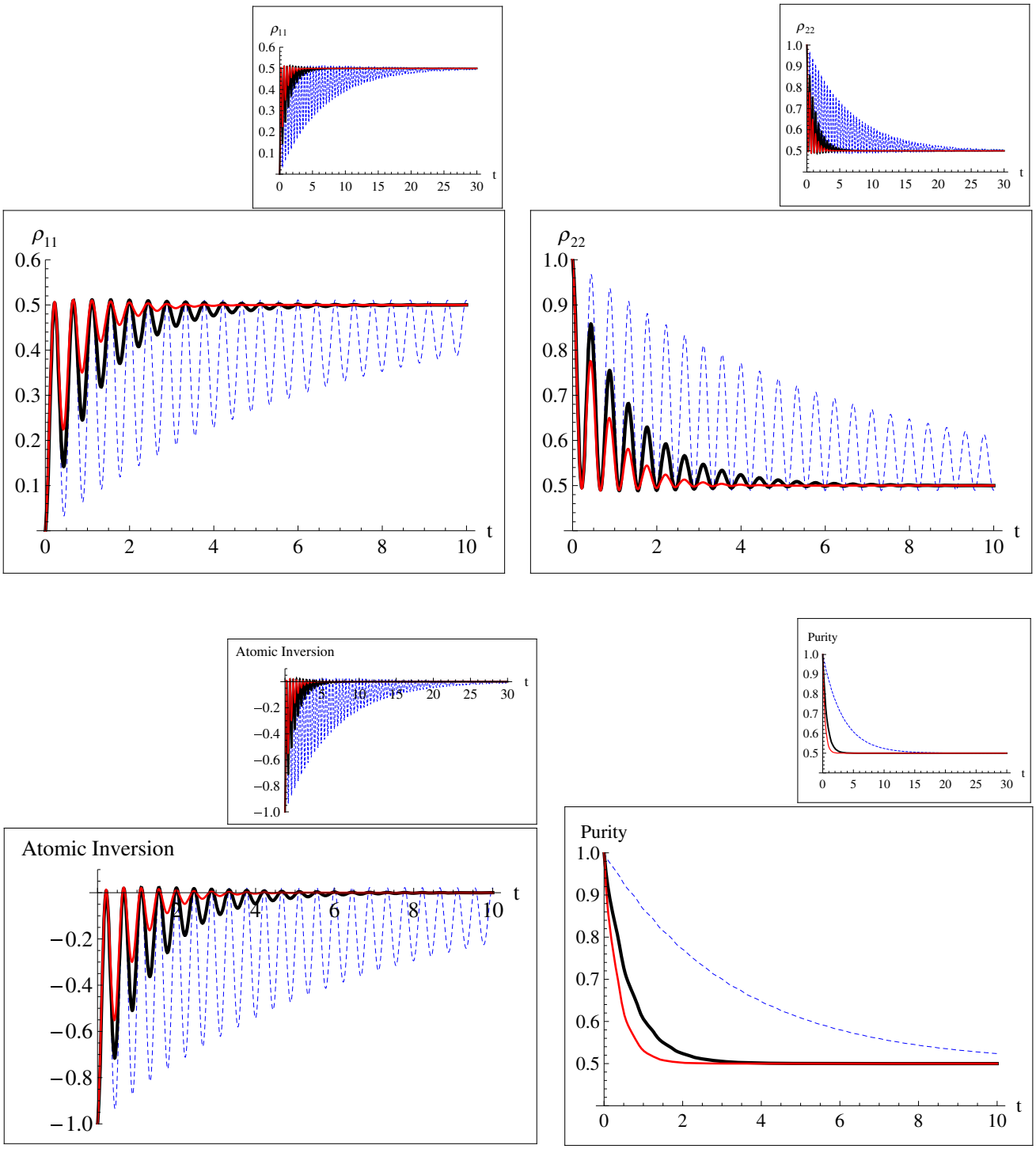

Figure 1. The effects of α_{12}, α_{21} and γ on $\rho_{11}(t)$, $\rho_{22}(t)$, $\rho_z(t)$ and $P_A(t)$ when $\theta = 0$, $\varphi = 0$, $\Omega = 10$ and $\Delta = 10$, where blue dotted, black and red curves correspond, respectively, to $\gamma = \eta = 0.1$, 0.5 and 0.9.

lines (long-lived quantum coherence). With regard to the purity curve $P_A(t)$, they start from their maximum value at $P_A(t) = 1$, then, suddenly and quickly, the curves decrease to a decaying state. Note that the effect of Δ on $P_A(t)$ are small, as all the curves of the purity are close to each other. They become fixed at $P_A(t) = 0.5$ (the completely mixed state, long-lived quantum coherence). In figure 5, we investigate the effects of Ω on $\rho_{11}(t)$, $\rho_{22}(t)$, $\rho_z(t)$ and $P_A(t)$, when $\Delta = 10$ and $\alpha_{12} = \alpha_{21} = \gamma = 0.3$. At $\Omega = 5$, 15 and 25, it can be noticed that,

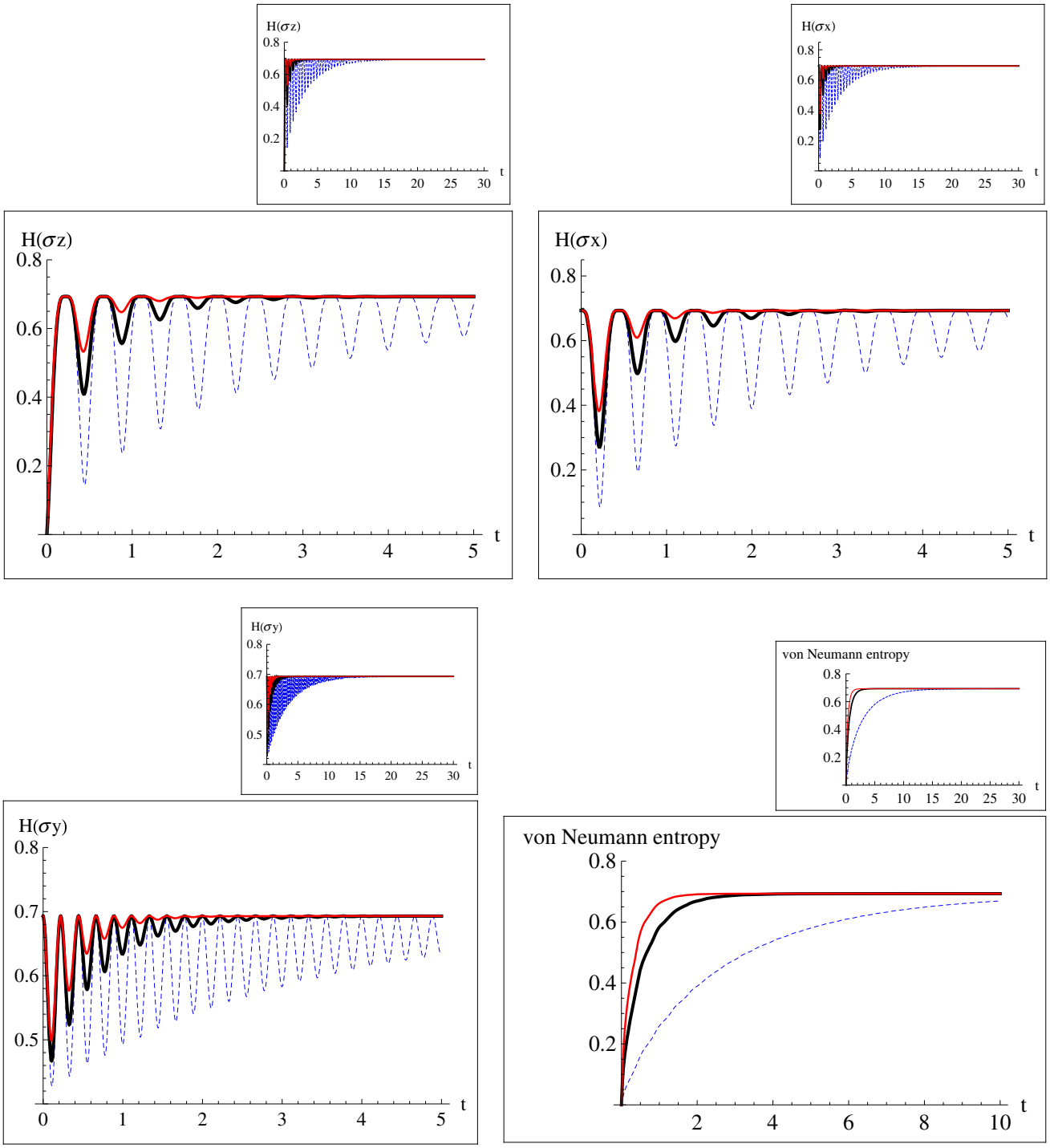

Figure 2. The effects of α_{12}, α_{21}, γ on $S(t)$, and $H(\sigma_x)$, $H(\sigma_y)$ and $H(\sigma_z)$, of the semiconductor quantum dot, when $\theta = 0$, $\varphi = 0$, $\Omega = 10$ and $\Delta = 10$, where blue dotted, black and red curves correspond, respectively, to $\gamma = \eta = 0.1$, 0.5 and 0.9.

with the increase in Ω, the maximum values of the curves $\rho_{11}(t)$ and $\rho_z(t)$ increase, while the minimum values of the curves $\rho_z(t)$ are greatly reduced first, then these minimum values continue to decrease but slightly. With the passing of time and increasing Ω, the oscillation amplitudes of all the curves, $\rho_{11}(t)$ and $\rho_{22}(t)$, $\rho_z(t)$, decrease until they finally stabilise at $\rho_{11}(t) = 0.4$, $\rho_{11}(t) = 0.5$ and $\rho_z(t) = 0$. In this case, it can also be observed that the effect of Ω on $P_A(t)$ are small. Finally, the curves from the beginning are in a state of decay, until they settle in the completely mixed state ($P_A(t) = 0.5$).

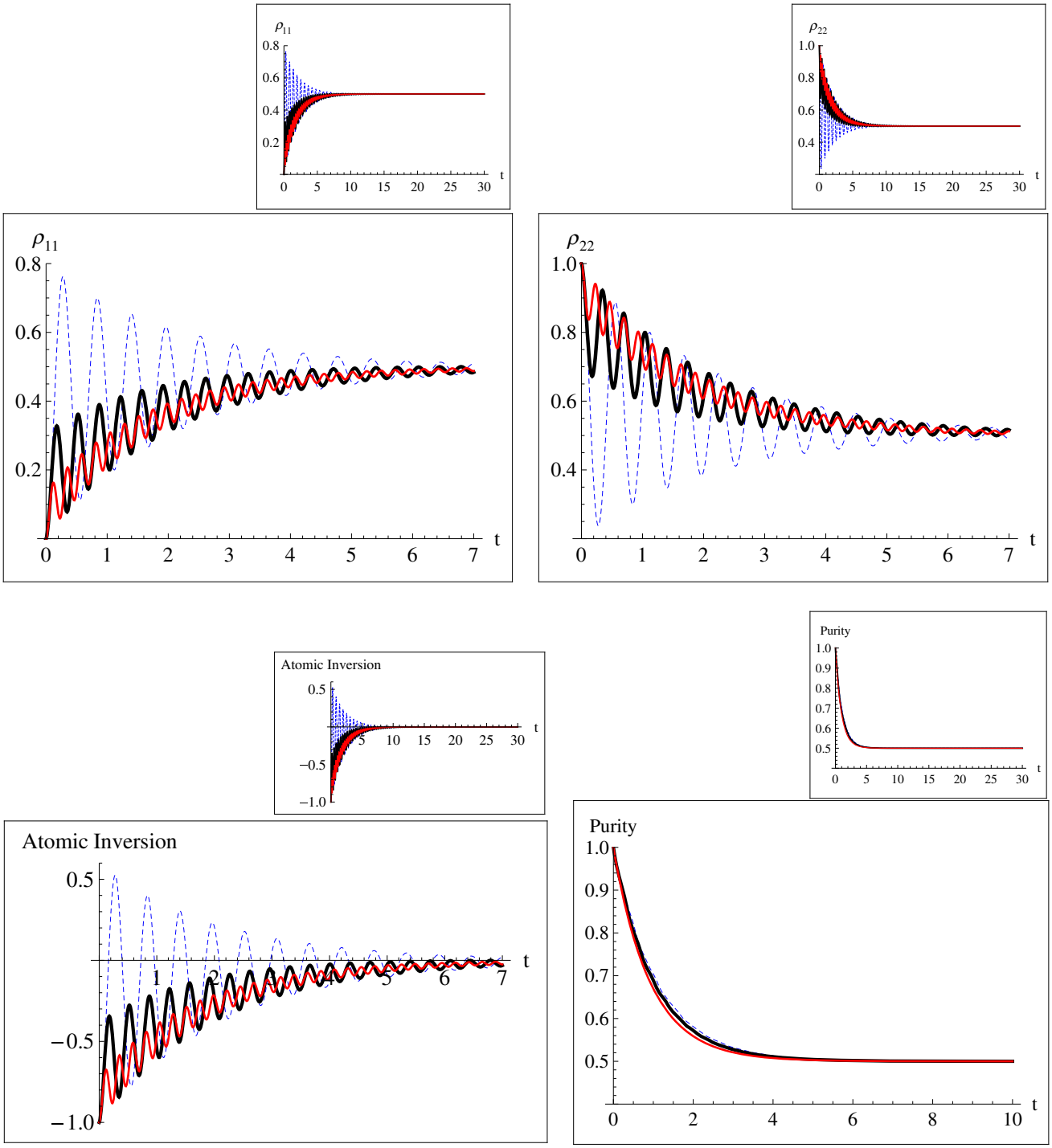

Figure 3. The effects of Δ on $\rho_{11}(t)$ and $\rho_{22}(t)$, $\rho_z(t)$, $P_A(t)$, when $\theta = 0$, $\varphi = 0$, $\Omega = 10$ and $\gamma = \eta = 0.3$, where blue dotted, black and red curves correspond, respectively, to $\Delta = 5$, 15 and 25.

3.2 *The information entropies and the von Neumann entropy*

There are different definitions of the entropy, for instance, the information entropy (the Shannon entropy) [86], the Rényi entropy [87], Hartley entropy [88], etc. We used the information entropy because it has unique properties which make it very useful and vital in many applications, such as statistical thermodynamics, and for constructing error-correcting codes [89], which are crucial for transmissions to and from space vehicles and many other communications systems. In accordance

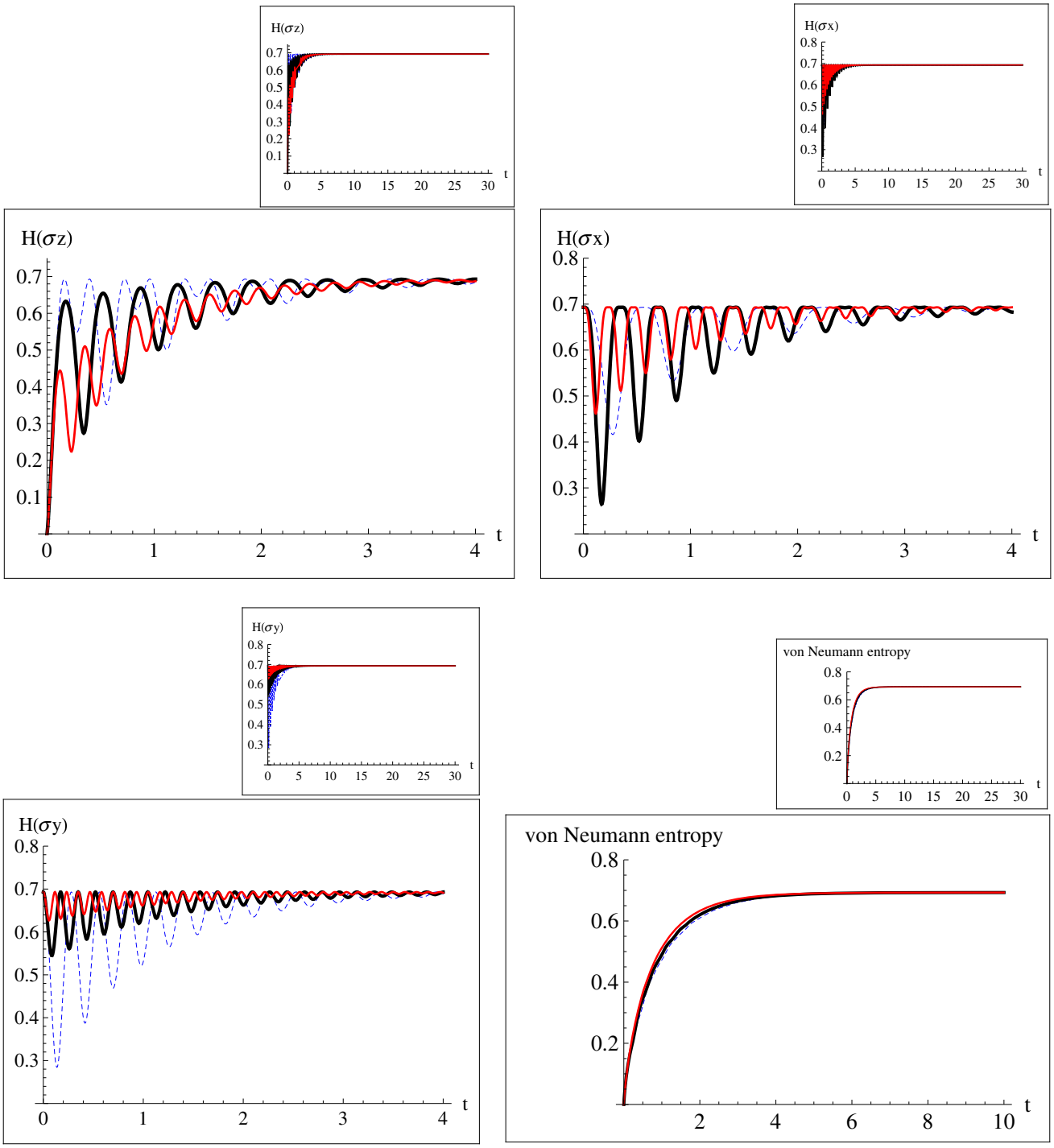

Figure 4. The effects of Δ on $S(t)$ and $H(\sigma_x)$, $H(\sigma_y)$ and $H(\sigma_z)$ of the semiconductor quantum dot, when $\Omega = 10$ and $\alpha_{12} = \alpha_{21} = \gamma = 0.3$ where the blue dotted, black and red curves correspond, respectively, to $\Delta = 5$, 15 and 25.

with the mathematical calculations in §2, this subsection presents the time evolution of the information entropies, $H(\sigma_x)$, $H(\sigma_y)$ and $H(\sigma_z)$, of the atomic operators σ_x, σ_y and σ_z, which are defined as follows [71,72,90]:

$$H(\sigma_\gamma) = -\sum_{k=1}^{n} P_k(\sigma_\gamma) \ln P_k(\sigma_\gamma), \quad \gamma = x, y, z, \quad (22)$$

where the probability distribution for n possible outcomes of measurements for an arbitrary quantum state of the operator σ_γ is

$$P_k(\sigma_\gamma) = \langle \Psi_{\gamma k} | \rho(t) | \Psi_{\gamma k} \rangle \quad (23)$$

and $|\Psi_{\gamma k}\rangle$ is the eigenvector of the operator σ_γ:

$$\sigma_\gamma |\Psi_{\gamma k}\rangle = \nu_{\gamma k} |\Psi_{\gamma k}\rangle,$$

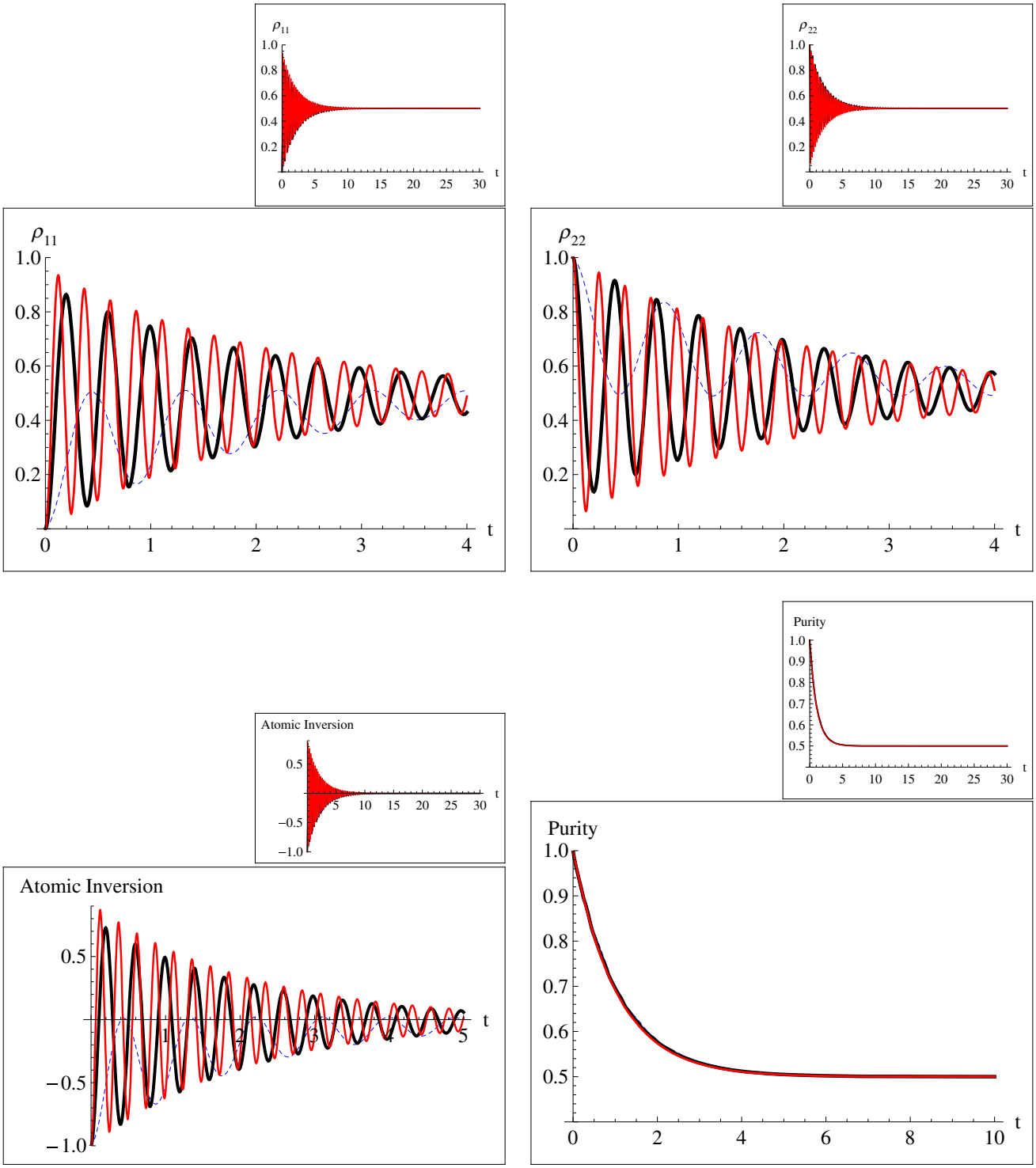

Figure 5. The effects of Ω on $\rho_{11}(t)$, $\rho_{22}(t)$, $\rho_z(t)$ and $P_A(t)$ when $\theta = 0$, $\varphi = 0$, $\Delta = 10$ and $\gamma = \eta = 0.3$, where the blue dotted, black and red curves correspond, respectively, to $\Omega = 5$, 15 and 25.

$$\gamma = x, y, z, \quad k = 1, 2, ..., n, \tag{24}$$

where $\nu_{\gamma k}$ is the eigenvalue of the atomic operator σ_γ.

As the operators σ_γ ($\gamma = x, y, z$) satisfy the commutation relations (4), then some kind of relationships is expected between their corresponding entropies $H(\sigma_\gamma)$ defined by eq. (22) and this will be explained now.

Using quantum entropy theory [91], an optimal entropic uncertainty relation was recently studied for sets of $M + 1$ complementary observables with non-degenerate eigenvalues in an even M-dimensional

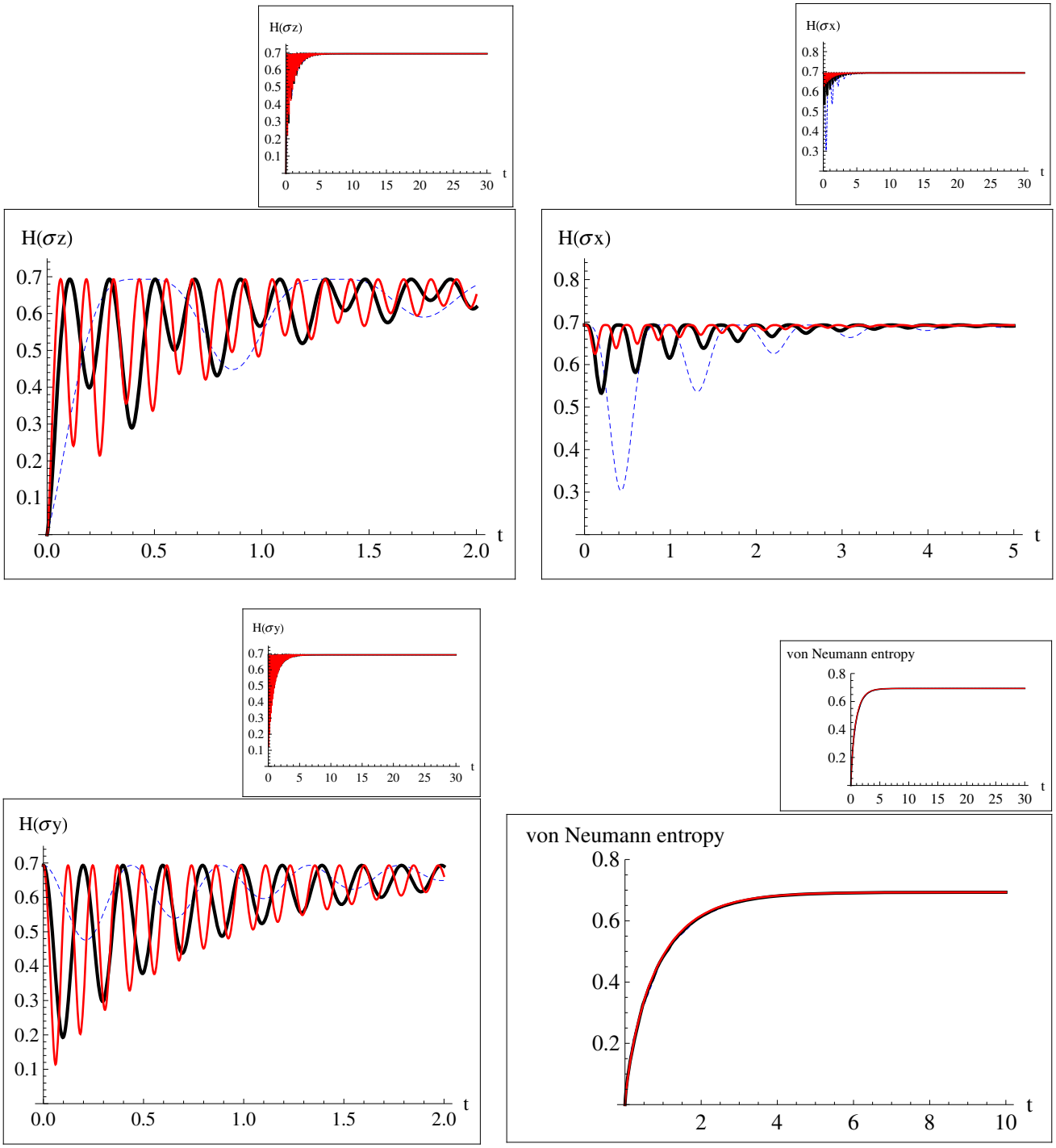

Figure 6. The effects of Ω on $S(t)$, and $H(\sigma_x)$, $H(\sigma_y)$ and $H(\sigma_z)$ of the semiconductor quantum dot when $\Delta = 10$ and $\alpha_{12} = \alpha_{21} = \gamma = 0.3$ where the blue dotted, black and red curves correspond, respectively, to $\Omega = 5$, 15 and 25.

Hilbert space, and it has been concluded that it takes the following formula:

$$\sum_{\gamma=1}^{M+1} H(\sigma_\gamma) \geq \frac{M}{2} \ln\left(\frac{M}{2}\right) + \left(1+\frac{M}{2}\right) \ln\left(1+\frac{M}{2}\right). \tag{25}$$

In the case of a two-level atom, $M = 2$, from eq. (25), we can observe that the information entropies of the operators σ_x, σ_y and σ_z satisfy the following inequality:

$$H(\sigma_x) + H(\sigma_y) \geq 2\ln(2) - H(\sigma_z). \tag{26}$$

Also, inequality (26) may be written as

$$\delta H(\sigma_x)\delta H(\sigma_y) \geq \frac{4}{|\delta H(\sigma_z)|}, \tag{27}$$

where $\delta H(\sigma_\alpha) = \exp[H(\sigma_\alpha)]$.

Inequality (26) will be clarified later through figures and discussion. Also we study the time evolution of the von Neumann entropy, $S(t)$, which is defined as [90]

$$\begin{aligned} S(t) &= -\mathrm{Tr}(\hat{\rho}(t)\ln\hat{\rho}(t)) \\ &= -(\delta_1 \ln \delta_1 + \delta_2 \ln \delta_2), \end{aligned} \tag{28}$$

where

$$\begin{aligned} \delta_{1,2} &= \frac{1}{2}\left\{1 \pm \sqrt{1 - 4(\rho_{11}\rho_{22} - |\rho_{12}|^2}\right\} \\ &= \frac{1}{2} \pm \sqrt{\langle\sigma_x\rangle^2 + \langle\sigma_y\rangle^2 + \langle\sigma_z\rangle^2}. \end{aligned} \tag{29}$$

In the numerical results, we also consider the relative phase between the excited and the ground states $\varphi = 0$ and the initial coherence of the two levels $\theta = 0$. Here, we can clearly see also the emergence of the phenomenon of long-lived quantum coherence in all the curves, which obviously manifest in the curves of the von Neumann entropy. In figure 2, we investigate the effects of α_{12}, α_{21} and γ on $S(t)$, and $H(\sigma_x)$, $H(\sigma_y)$ and $H(\sigma_z)$, of the semiconductor quantum dot, when $\Omega = 10$ and $\Delta = 10$. At $\alpha_{12} = \alpha_{21} = \gamma = 0.1$, $\alpha_{12} = \alpha_{21} = \gamma = 0.5$ and $\alpha_{12} = \alpha_{21} = \gamma = 0.9$, the curves of $H(\sigma_x)$ and $H(\sigma_y)$ start from their maximum value at $H(\sigma_x) = H(\sigma_y) = 0.7$, while the curves of $H(\sigma_z)$ start with its minimum value at $H(\sigma_z) = 0$. In the beginning, the curves of $H(\sigma_x)$, $H(\sigma_y)$ and $H(\sigma_z)$ go in fluctuated ups and downs, the intensity and amplitudes of these oscillations are large and clear. After a certain period of time, we note that the intensity, amplitudes and the number of oscillations decrease significantly, until the curves become a straight line. It draws clearly the phenomenon of long-lived quantum coherence. We note that by increasing α_{12}, α_{21} and γ, the curves become fixed faster than before. As for the von Neumann entropy curves, $S(t)$, they start from their minimum value at $S(t) = 0$, then suddenly increase plainly. The increase of the maximum values of von Neumann entropy curves become greater and faster, by increasing α_{12}, α_{21} and γ. Then the curves become fixed at their maximum value at $S(t) = 0.7$. These curves remain fixed even over time, and also remain fixed even if α_{12}, α_{21} and γ increase, depicting a long-lived quantum coherence. In figure 4, we investigate the effects of Δ on $S(t)$ and $H(\sigma_x)$, $H(\sigma_y)$ and $H(\sigma_z)$, of the semiconductor quantum dot, when $\Omega = 10$ and $\alpha_{12} = \alpha_{21} = \gamma = 0.3$. At $\Delta = 5$, 15 and 25, the intensity and amplitudes of the oscillations of the curves $H(\sigma_x)$, $H(\sigma_y)$ and $H(\sigma_z)$ are initially large and clear. It is observed that, by increasing Δ, the maximum values of $H(\sigma_z)$ decrease and the minimum values of $H(\sigma_y)$ increase, while the maximum values of $H(\sigma_x)$ hesitate between the increase and the decrease, until all the curves, $H(\sigma_x)$, $H(\sigma_y)$ and $H(\sigma_z)$, become fixed, without any effect of Δ and time. With respect to the von Neumann entropy curves, $S(t)$, they start from their minimum value at $S(t) = 0$, then, suddenly and quickly, the curves increase until they reach their maximum value. At this maximum value, the curves are stabilised, and there is no change in their behaviour, no matter how long. The effect of the change of Δ is very weak, as the curves are almost integrated with each other (long-lived quantum coherence). In figure 6, we investigate the effects of Ω on $S(t)$, and $H(\sigma_x)$, $H(\sigma_y)$ and $H(\sigma_z)$, of the semiconductor quantum dot, when $\Delta = 10$ and $\alpha_{12} = \alpha_{21} = \gamma = 0.3$. At $\Omega = 5$, 15 and 25, the curves of $H(\sigma_x)$ and $H(\sigma_y)$ ($H(\sigma_z)$) start from their maximum values (minimum value) until they reach minimum values (maximum value). In the beginning, with the increase of Ω, the number of oscillations increases significantly, especially in the curves of $H(\sigma_y)$ and $H(\sigma_z)$, but after a period of time, all the curves reach the fixed state at their maximum value at $H(\sigma_x) = H(\sigma_y) = H(\sigma_z) = 0.7$. As for the curve of the von Neumann entropy, $S(t)$, we also note that the effect of Ω on the von Neumann entropy is slight, and that the curve initially increases rapidly for its maximum value, and then becomes fixed, drawing again a long-lived quantum coherence.

By referring to figures 1–6 with a time scale from 0 to 30, we find that with the increase of α_{12}, α_{21} and γ, the curves of $\rho_{11}(t)$ and $\rho_{22}(t)$ and $\rho_z(t)$ reach the case of long-lived quantum coherence at $t = 30$, while the curves of $P_A(t)$, $S(t)$ and $H(\sigma_x)$, $H(\sigma_y)$, $H(\sigma_z)$ reach the case of long-lived quantum coherence at $t = 14$. We also find that with the increase of Δ and Ω, the curves of $\rho_{11}(t)$, $\rho_{22}(t)$ and $\rho_z(t)$ reach the case of long-lived quantum coherence at $t = 10$, while the curves of $P_A(t)$, $S(t)$, $H(\sigma_x)$, $H(\sigma_y)$ and $H(\sigma_z)$ reach the case of long-lived quantum coherence at $t = 5$. We note that the time of arrival to long-lived quantum coherence case does not change with the increase of Δ and Ω. We also note that the curves of $P_A(t)$, $S(t)$, $H(\sigma_x)$, $H(\sigma_y)$ and $H(\sigma_z)$ reach the case of long-lived quantum coherence at the same time. This is a typically expected behaviour, as all these curves measure to what degree the atom is affected by the field. We observe that when the entropies increase, the atom is increasingly affected by the field, and the purity decreases at the same time. Thus, if the entropies reach a state of stability at a high value, the purity curve would reach stability at a low value.

In the zeroth approximation in $\max\{\alpha_{12}, \alpha_{21}, \gamma\}/\Omega$, we can calculate the probability of finding the quantum dot in the excited state at an arbitrary time $\rho_{22}(t)$ as follows:

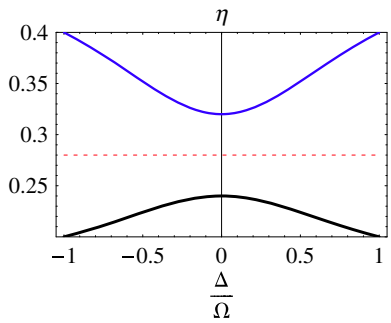

Figure 7. The dephasing rate η of Rabi oscillations vs. the normalised detuning from the resonance Δ/Ω, where the black, red dotted and blue curves correspond, respectively, to $\chi = 0.32$, $\gamma = 0$ ($\chi > \gamma$), $\chi = 0.28$, $\gamma = 0.28$ ($\chi = \gamma$) and $\chi = 0.16$, $\gamma = 0.8$ ($\chi < \gamma$).

$$\rho_{22}(t) = \langle 2|\,\rho\,|2\rangle$$
$$= \frac{1}{2}(1 - \{\exp(-\eta t)\sin^2(\Phi)\cos(\zeta t) + \cos(\Phi)$$
$$\times [\cos(\Phi)\exp(-\epsilon t) - \tau(1 - \exp(-\epsilon t))]\}), \tag{30}$$

where $\zeta = \sqrt{\Delta^2 + \Omega^2}$ is the generalised Rabi frequency, $\sin(\Phi) = \Omega/\zeta$, $\cos(\Phi) = \Delta/\zeta$ and $\tau = (\alpha_{12} - \alpha_{21})\cos(\Phi)/\epsilon$.

Also,

$$\epsilon = \chi + \frac{1}{2}(\gamma - \chi)\sin(\Phi), \tag{31}$$

$$\eta = \frac{1}{2}(\chi) + \frac{1}{4}(\chi - \gamma)\frac{\Omega^2}{\zeta^2}, \tag{32}$$

$$\chi = \alpha_{12} + \alpha_{21}. \tag{33}$$

Rabi oscillations of the excited state of the quantum dot occur with the frequency ζ and damp at the rate η (eq. (32), figure 7). In figure 7, we investigate the effect of normalised detuning from the resonance Δ/Ω, on the dephasing rate η, at $\chi = 0.32$, $\gamma = 0$ ($\chi > \gamma$), $\chi = 0.28$, $\gamma = 0.28$ ($\chi = \gamma$) and $\chi = 0.16$, $\gamma = 0.8$ ($\chi < \gamma$). From eq. (32), we can observe the dependence of the dephasing rate of Rabi oscillations on detuning from the resonance Δ/Ω, which is determined by the ratio between the total rates of photon radiative and phonon radiationless transitions χ, and pure dephasing γ. When $\chi > \gamma$, as the detuning parameter increases, the dephasing rate decreases. However, when $\chi < \gamma$, the increase in the detuning parameter is followed by an increase in the dephasing rate and when $\chi = \gamma$, the dephasing rate is completely independent of the detuning parameter.

4. Conclusion

In this paper, we analytically solved the system of two-level semiconductor quantum dot. We discussed the effects of α_{12}, α_{21}, γ, Δ and Ω on $\rho_{11}(t)$ and $\rho_{22}(t)$, $\rho_z(t)$, $P_A(t)$, $S(t)$, and $H(\sigma_x)$, $H(\sigma_y)$ and $H(\sigma_z)$. It was observed that with the increase in α_{12}, α_{21}, the values of γ, Δ and Ω, the number of oscillations and their intensity were initially very large. However, after a period of time, all curves, $\rho_{11}(t)$, $\rho_{22}(t)$, $\rho_z(t)$, $P_A(t)$, $S(t)$, $H(\sigma_x)$, $H(\sigma_y)$ and $H(\sigma_z)$, became fixed. The curves reached the fixed state rapidly by increasing α_{12}, α_{21}, γ, Δ and Ω. On the other hand, we observed the decay in the purity curve and the long-lived quantum coherence phenomenon in all the curves, especially in the purity curves and the von Neumann entropy curves. Besides, the curves of the purity mirrored the von Neumann entropy curves through a straight line parallel to the axis of t. We can control the behaviour of the system by changing the parameters. Thus, the results of the study have revealed the time interval in which we can predict the emergence of the long-lived quantum coherence. Accordingly, we can identify the interval wherein the effect of the field on the system remains fixed and our information about the system can thereby be stable. Being vitally applied in precision measurement, quantum networks [92–94] and atomic interferometric sensors, controlling or predicting the emergence of long-lived quantum coherence can, consequently, help us in various fields of applications. Our results can be specifically applied to gallium arsenide (GaAs), as it is the compound represented in our problem. Among the advantageous properties of GaAs are its high saturated electron speed and its low-field electron mobility which are much greater than those of silicon [3–6]. In fact, the carrier mobility of GaAs can be six times higher than that of silicon. So most of the carrier devices in GaAs are faster and less noisy than in silicon. That is why gallium arsenide transistors can operate efficiently at frequencies over 250 GHz. Besides, unlike the indirect band gap of silicon, GaAs has a direct band gap which allows it to absorb and emit light effectively. Moreover, due to their wider energy band gaps, GaAs devices have efficient resistance to both overheating and radiation damage which make GaAs crucially vital for high power applications [3–7]. For instance, it is used in nuclear bombs to preserve the stability of the crystal structure. Hence, our results can even be more significant as it explores the information entropy of a compound like GaAs which has various high-power and sensitive applications. Highly sensitive and precise as they are, being able to predict the time interval in which our information about this system (GaAs) becomes stable could increase the stability and controllability of its vast applications, such as in optical

applications, high-performance transistors [18,25,26], medical imaging, quantum computing, solar cells, LED lamps and diode lasers. To conclude, this paper links the work on quantum dots with other research streams in biology, medicine, industry, and others, which are enjoying growing interest in research on nanotechnology, thus uncovering new connections and applications to explore. So, we recommend further mathematical exploration, such as handling more complicated systems and higher levels of atoms, which would uncover more properties and phenomena of quantum dots.

Acknowledgements

The author thanks the editor and the reviewer for giving him the chance to revise and improve this paper. The author deeply appreciates the profound comments and the constructive ideas of the reviewer which add a lot to the manuscript.

References

[1] J B Johnson, *Phys. Rev.* **32**, 97 (1928)
[2] M Mogi, M Kawamura, R Yoshimi, A Tsukazaki, Y Kozuka, N Shirakawa, K S Takahashi, M Kawasaki and Y Tokura, *Nature Mater.* **16**, 516 (2017)
[3] B G Yacobi, *Semiconductor materials: An introduction to basic principles* (Springer, New York, 2003)
[4] A A Balandin and K L Wang, *Handbook of semiconductor nanostructures and nanodevices* (American Scientific Publishers, 2006), a set of 5 volumes
[5] J Turley, *The essential guide to semiconductors* (Prentice Hall, PTR, Upper Saddle River, 2002)
[6] Y Peter and C Manuel, *Fundamentals of semiconductors: Physics and materials properties* (Springer, New York, 2004)
[7] S Adachi, *The handbook on optical constants of semiconductors: In tables and figures* (World Scientific Publishing, Singapore, 2012)
[8] R F Cregan, B J Mangan, J C Knight, T A Birks, P St J Russell, P J Roberts and D C Allan, *Science* **285**, 1537 (1999)
[9] V Srikant and D R Clarke, *J. Appl. Phys.* **83**, 5447 (1998)
[10] K Zhang, K Deng, J Li, H Zhang, W Yao, J Denlinger, Y Wu, W Duan and S Zhou, *Phys. Rev. Mater.* **2**, 054603 (2018)
[11] J Gao, K Kempa, M Giersig, E M Akinoglu, B Han and R Li, *Adv. Phys.* **65**, 553 (2016)
[12] Y Volpez, D Loss and J Klinovaja, *Phys. Rev. B* **96**, 085422 (2017)
[13] W A Benalcazar, B A Bernevig and T L Hughes, *Science* **357**, 61 (2017)
[14] S M Sze and K K Ng, *Physics of semiconductor devices*, 3rd Edn (John Wiley and Sons, New York, 2006)
[15] C Kittel, *Introduction to solid state physics*, 7th Edn (Wiley, New York, 1995)
[16] L E Brus, *J. Phys. Chem. Solids* **59**, 459 (1998)
[17] J W Allen, *Nature* **187**, 403 (1960)
[18] R Stoklas, D Gregusovl, M Blaho, K Frhlich, J Novlk, M Matys, Z Yatabe, P Kordoš and T Hashizume, *Semicond. Sci. Technol.* **32**, 045018 (2017)
[19] T J Dhilip Kumar, P Tarakeshwar and N Balakrishnan, *J. Chem. Phys.* **128**, 194714 (2008)
[20] S Adachi, *GaAs and related materials: Bulk semiconducting and superlattice properties* (World Scientific, Singapore, 1994)
[21] J Orton, *The story of semiconductors* (Oxford University Press, Oxford, 2004).
[22] G Busch, *Eur. J. Phys.* **10**, 254 (1989)
[23] P R Morris, *A history of the world semiconductor industry* (IET, 1990)
[24] F Braun, *Planar microwave engineering: A practical guide to theory, measurement, and circuits* (Cambridge University Press, 2004)
[25] Z Li, M Khaled Husain, H Yoshimoto, K Tani, Y Sasago, D Hisamoto, J D Fletcher, M Kataoka, Y Tsuchiya and S Saito, *Semicond. Sci. Technol.* **32**, 075001 (2017)
[26] W Shockley, *Electrons and holes in semiconductors: With applications to transistor electronics* (R. E. Krieger Pub., Melbourne, 1950)
[27] C H Sterling, *Military communications: From ancient times to the 21st century* (ABC-CLIO, Inc., California, 2008)
[28] S Gangasani, *Eng. Technol.* **5**, 8128 (2007)
[29] A Zora, C Simserides and G P Triberis, *J. Phys.: Condens. Matter* **19**, 406201 (2007)
[30] C D Simserides, U Hohenester, G Goldoni and E Molinari, *Phys. Status Solidi B* **224**, 745 (2001)
[31] C D Simserides, U Hohenester, G Goldoni and E Molinari, *Mater. Sci. Eng. B* **80**, 266 (2001)
[32] A Hartmann, Y Ducommun, E Kapon, U Hohenester, C Simserides and E Molinari, *Phys. Status Solidi A* **178**, 283 (2000)
[33] C Simserides, U Hohenester, G Goldoni and E Molinari, *Local optical absorption by confined excitons in single and coupled quantum dots* (Springer, Berlin, 2001)
[34] G B Abdullayev, T D Dzhafarov and S Torstveit (Translator), *Atomic diffusion in semiconductor structures* (Gordon & Breach Science Pub., 1987)
[35] M Cutler and N F Mott, *Phys. Rev.* **181**, 1336 (1969)
[36] I V Martynenko, A P Litvin, F Purcell-Milton, A V Baranov, A V Fedorov and Y K Gun'ko, *Appl. Mater. Chem. B* **5**, 6701 (2017)
[37] M Sabaeian and A Khaledi-Nasab, *Appl. Opt.* **51**, 4176 (2012)
[38] G A M Safar, W N Rodrigues, L A Cury, H Chacham, M V B Moreira, S L S Freire and A G de Oliveira, *Appl. Phys. Lett.* **71**, 521 (1997)
[39] D Leonard, S Fafard, K Pond, Y H Zhang, J L Merz and P M Petroff, *J. Vac. Sci. Technol. B* **12**, 2516 (1994)
[40] Mei-Ying Kong, Xiao-Liang Wang, Dong Pan and Yi-Ping Zeng, *J. Appl. Phys.* **86**, 1456 (1999)

[41] R C Ashoori, *Nature* **379**, 413 (1996)
[42] M A Kastner, *Phys. Today* **46**, 24 (1993)
[43] C D Simserides, U Hohenester, G Goldoni and E Molinari, *Phys. Rev. B* **62**, 13657 (2000)
[44] A Khaledi-Nasab, M Sabaeian, M Sahrai and V Fallahi, *J. Opt.* **16**, 55517 (2014)
[45] H Y Ramerez, J Flrez and A S Camacho, *Phys. Chem.* **17**, 23938 (2015)
[46] D Pan, Y P Zeng, J Wu, H M Wang, C H Chang, J M Li and M Y Kong, *Appl. Phys. Lett.* **70**, 2440 (1997)
[47] D Pan, Y P Zeng, M Y Kong, J Wu, Y Q Zhu, C H Zhang, J M Li and C Y Wang, *Electron. Lett.* **32**, 1726 (1996)
[48] J L Liu, W G Wu, A Balandin, G L Jin and K L Wang, *Appl. Phys. Lett.* **74**, 185 (1999)
[49] J Phillips, K Kamath and P Bhattacharya, *Appl. Phys. Lett.* **72**, 2020 (1998)
[50] A Zora, C Simserides and G Triberis, *Phys. Status Solidi A* **202**, 619 (2005)
[51] A Zora, C Simserides and G P Triberis, *J. Phys.: Conf. Ser.* **245**, 012037 (2010)
[52] C Simserides, A Zora and G Triberis, *Int. J. Mod. Phys. B* **21**, 1649 (2007)
[53] A Zora, C Simserides and G Triberis, *AIP Conf. Proc.* **893**, 893 (2007)
[54] A Zora, C Simserides and G Triberis, *Int. J. Mod. Phys. B* **18**, 3717 (2004)
[55] T Krnhenmann, L Ciorciaro, C Reichl, W Wegscheider, L Glazman, T Ihn and K Ensslin, *New J. Phys.* **19**, 023009 (2017)
[56] A Hofmann, V F Maisi, J Basset, C Reichl, W Wegscheider, T Ihn, K Ensslin and C Jarzynski, *Phys. Status Solidi B* **254**, 1600546 (2017)
[57] A Stockklauser, P Scarlino, J V Koski, S Gasparinetti, C K Andersen, C Reichl, W Wegscheider, T Ihn, K Ensslin and A Wallraff, *Phys. Rev.* **7**, 011030 (2017)
[58] A Hofmann, V F Maisi, T Krnhenmann, C Reichl, W Wegscheider, K Ensslin and T Ihn, *Phys. Rev. Lett.* **119**, 176807 (2017)
[59] S Xu, A L Dadlani, S Acharya, P Schindler and F B Prinz, *Appl. Surface Sci.* **367**, 500 (2016)
[60] I A Gorbachev, I Yu Goryacheva and E G Glukhovskoy, *Bionanoscience* **6**, 153 (2016)
[61] M Achermann, M A Petruska, S A Crooker and V I Klimov, *J. Phys. Chem. B* **107**, 13782 (2003)
[62] S Coe-Sullivan, J S Steckel, W-K Woo, M G Bawendi and V Bulović, *Adv. Funct. Mater.* **15**, 1117 (2005)
[63] R van den Berg, G P Brandino, O El Araby, R M Konik, V Gritsev and J-S Caux, *Phys. Rev. B* **90**, 155117 (2014)
[64] A J Nozik, *Annu. Rev. Phys. Chem.* **52**, 193 (2001)
[65] K Chang and Jian-Bai Xia, *Phys. Rev. B* **57**, 9780 (1998)
[66] C Chang-Hasnain and S Lien Chuan, *J. Lightw. Technol.* **24**, 4642 (2007)
[67] D A M Abo-Kahla, *Appl. Math. Inform. Sci.* **10**, 1 (2016)
[68] D A M Abo-Kahla, M Abdel-Aty and A Farouk, *Int. J. Theor. Phys.* **57**, 2319 (2018)
[69] G Ye, C Pan, X Huang, Z Zhao and J He, *Int. J. Bifurc. Chaos* **28**, 1850010 (2018)
[70] I S Gomez, M Losada and O Lombardi, *Entropy* **19**, 205 (2017)
[71] D A M Abo-Kahla and M Abdel-Aty, *Int. J. Quantum Inform.* **13**, 1550042 (2015)
[72] D A M Abo-Kahla, *Nonlinear Dyn.* **94**, 1689 (2018)
[73] A Löffler, A Forchel, P Michler, S M Ulrich, S Ates and S Reitzenstein, *Phys. Rev. Lett.* **106**, 247402 (2011)
[74] A Ulhaq, S Weiler, C Roy, S M Ulrich, M Jetter, S Hughes and P Michler, *Opt. Express* **21**, 4382 (2013)
[75] P S Dara, *Phys. Rev. Lett.* **110**, 217401 (2013)
[76] K Fujii, *J. Mod. Phys.* **08**(**12**), 2042 (2017)
[77] B Thimmel, P Nalbach and O Terzidis, *Eur. Phys. J. B* **9**, 207 (1999)
[78] L W Casperson, *Phys. Rev. A* **46**(**1**), 401 (1992)
[79] C Majenz, T Albash, H P Breuer and D A Lidar, *Phys. Rev. A* **88**(**1**), 012103 (2013)
[80] O Marlan Scully and M Suhail Zubairy, *Quantum optics* (Cambridge University Press, Cambridge, 1997)
[81] V Farra and I Pšenčík, *J. Acoust. Soc. Am.* **114**(**3**), 1366 (2003)
[82] G Panitchayangkoon, D Hayes, K A Fransted, J R Caram, E Harel, J Wen, R E Blankenship and G S Engel, *Proc. Natl Acad. Sci. USA* **107**(**29**), 12766 (2010)
[83] M Xin, W S Leong, Z Chen and S-Y Lan, *Phys. Rev. Lett.* **122**, 163901 (2019)
[84] S Koyu and T V Tscherbul, *Phys. Rev. A* **98**, 023811 (2018)
[85] H-G Duan, V I Prokhorenko, R J Cogdell, K Ashraf, A L Stevens, E Wientjes, R Croce, M Thorwart and R J D Miller, *EPJ Web of Conferences* **205**, 09035 (2019)
[86] C E Shannon, *Bell System Tech. J.* **27**, 379 (1948)
[87] A Rényi, On Measures of Information and Entropy, in: *Proceedings of the 4th Berkeley Symposium on Mathematics, Statistics and Probability* (University of California Press, Berkeley and Los Angeles, 1960) pp. 547–561
[88] O Rioul and J C Magossi, *Entropy* **16**(**9**), 4892 (2014)
[89] R W Hamming, *Bell System Tech. J.* **29**(**2**), 147 (1950)
[90] T M El-Shahat, S Abdel-Khalek, M Abdel-Aty and A-S F Obada, *Chaos Solitons Fractals* **18**, 289 (2003)
[91] M F Fang, P Zhou and S Swain, *J. Mod. Opt.* **47**(**6**), 1043 (2000)
[92] A D Cronin, J Schmiedmayer and D E Pritchard, *Rev. Mod. Phys.* **81**, 1051 (2009)
[93] H J Kimble, *Nature* **453**, 1023 (2008)
[94] K Hammerer, A S Srensen and E S Polzik, *Rev. Mod. Phys.* **82**, 1041 (2010)